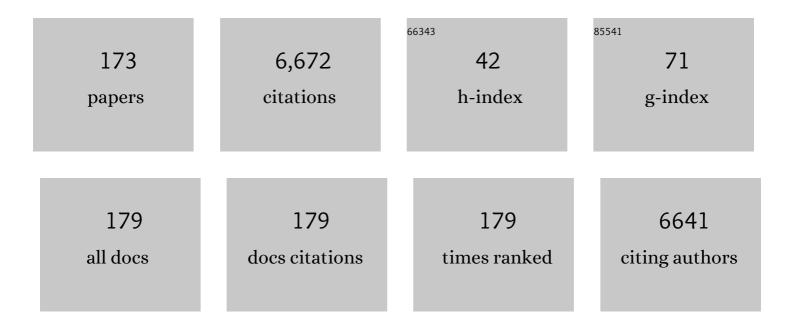
List of Publications by Year in descending order

Source: https://exaly.com/author-pdf/5629483/publications.pdf Version: 2024-02-01



VIVIIN HUANC

#	Article	lF	CITATIONS
1	Imaging synaptic density in the living human brain. Science Translational Medicine, 2016, 8, 348ra96.	12.4	343
2	Deficits in Prefrontal Cortical and Extrastriatal Dopamine Release in Schizophrenia. JAMA Psychiatry, 2015, 72, 316.	11.0	304
3	Assessing Synaptic Density in Alzheimer Disease With Synaptic Vesicle Glycoprotein 2A Positron Emission Tomographic Imaging. JAMA Neurology, 2018, 75, 1215.	9.0	304
4	Imaging robust microglial activation after lipopolysaccharide administration in humans with PET. Proceedings of the National Academy of Sciences of the United States of America, 2015, 112, 12468-12473.	7.1	265
5	Relationships between radiotracer properties and image quality in molecular imaging of the brain with positron emission tomography. Molecular Imaging and Biology, 2003, 5, 363-375.	2.6	202
6	Synthesis and Preclinical Evaluation of ¹¹ C-UCB-J as a PET Tracer for Imaging the Synaptic Vesicle Glycoprotein 2A in the Brain. Journal of Nuclear Medicine, 2016, 57, 777-784.	5.0	197
7	In vivo measurement of widespread synaptic loss in Alzheimer's disease with SV2A PET. Alzheimer's and Dementia, 2020, 16, 974-982.	0.8	170
8	Kinetic evaluation and test–retest reproducibility of [¹¹ C]UCB-J, a novel radioligand for positron emission tomography imaging of synaptic vesicle glycoprotein 2A in humans. Journal of Cerebral Blood Flow and Metabolism, 2018, 38, 2041-2052.	4.3	143
9	Rapid Changes in Cannabinoid 1 Receptor Availability in Cannabis-Dependent Male Subjects After Abstinence From Cannabis. Biological Psychiatry: Cognitive Neuroscience and Neuroimaging, 2016, 1, 60-67.	1.5	135
10	Brivaracetam, a selective highâ€affinity synaptic vesicle protein 2A (<scp>SV</scp> 2A) ligand with preclinical evidence of high brain permeability and fast onset of action. Epilepsia, 2016, 57, 201-209.	5.1	130
11	Comparative evaluation of serotonin transporter radioligands 11C-DASB and 11C-McN 5652 in healthy humans. Journal of Nuclear Medicine, 2004, 45, 682-94.	5.0	114
12	Synaptic Changes in Parkinson Disease Assessed with in vivo Imaging. Annals of Neurology, 2020, 87, 329-338.	5.3	112
13	Comparative Evaluation in Nonhuman Primates of Five PET Radiotracers for Imaging the Serotonin Transporters: [¹¹ C]McN 5652, [¹¹ C]ADAM, [¹¹ C]DASB, [¹¹ C]DAPA, and [¹¹ C]AFM. Journal of Cerebral Blood Flow and Metabolism, 2002, 22, 1377-1398.	4.3	111
14	Increased Nanoparticle Delivery to Brain Tumors by Autocatalytic Priming for Improved Treatment and Imaging. ACS Nano, 2016, 10, 4209-4218.	14.6	103
15	Preferential binding to dopamine D3 over D2 receptors by cariprazine in patients with schizophrenia using PET with the D3/D2 receptor ligand [11C]-(+)-PHNO. Psychopharmacology, 2016, 233, 3503-3512.	3.1	101
16	Recovery from chronic spinal cord contusion after nogo receptor intervention. Annals of Neurology, 2011, 70, 805-821.	5.3	87
17	PET imaging of synaptic density: A new tool for investigation of neuropsychiatric diseases. Neuroscience Letters, 2019, 691, 44-50.	2.1	85
18	Reduced Brain Cannabinoid Receptor Availability in Schizophrenia. Biological Psychiatry, 2016, 79, 997-1005.	1.3	83

#	Article	IF	CITATIONS
19	Synthesis and Evaluation of 11C-LY2795050 as a κ-Opioid Receptor Antagonist Radiotracer for PET Imaging. Journal of Nuclear Medicine, 2013, 54, 455-463.	5.0	80
20	Reduced Amygdala Serotonin Transporter Binding in Posttraumatic Stress Disorder. Biological Psychiatry, 2011, 70, 1033-1038.	1.3	79
21	Imaging the Cannabinoid CB1 Receptor in Humans with [¹¹ C] OMAR: Assessment of Kinetic Analysis Methods, Test–Retest Reproducibility, and Gender Differences. Journal of Cerebral Blood Flow and Metabolism, 2015, 35, 1313-1322.	4.3	79
22	Assessment of a white matter reference region for ¹¹ C-UCB-J PET quantification. Journal of Cerebral Blood Flow and Metabolism, 2020, 40, 1890-1901.	4.3	77
23	Synthesis and <i>in Vivo</i> Evaluation of a Novel PET Radiotracer for Imaging of Synaptic Vesicle Glycoprotein 2A (SV2A) in Nonhuman Primates. ACS Chemical Neuroscience, 2019, 10, 1544-1554.	3.5	70
24	Association of In Vivo κ-Opioid Receptor Availability and the Transdiagnostic Dimensional Expression of Trauma-Related Psychopathology. JAMA Psychiatry, 2014, 71, 1262.	11.0	67
25	Imaging Clutamate Homeostasis in Cocaine Addiction with the Metabotropic Clutamate Receptor 5 Positron Emission Tomography Radiotracer [11C]ABP688 and Magnetic Resonance Spectroscopy. Biological Psychiatry, 2014, 75, 165-171.	1.3	66
26	In vivo affinity of [18F]fallypride for striatal and extrastriatal dopamine D2 receptors in nonhuman primates. Psychopharmacology, 2004, 175, 274-286.	3.1	63
27	First-in-Human Evaluation of ¹⁸ F-SynVesT-1, a Radioligand for PET Imaging of Synaptic Vesicle Glycoprotein 2A. Journal of Nuclear Medicine, 2021, 62, 561-567.	5.0	60
28	Fluorinated Diaryl Sulfides as Serotonin Transporter Ligands:Â Synthesis, Structureâ^'Activity Relationship Study, and in Vivo Evaluation of Fluorine-18-Labeled Compounds as PET Imaging Agents. Journal of Medicinal Chemistry, 2005, 48, 2559-2570.	6.4	59
29	11C-GR103545, a radiotracer for imaging kappa-opioid receptors in vivo with PET: synthesis and evaluation in baboons. Journal of Nuclear Medicine, 2005, 46, 484-94.	5.0	59
30	In Vivo Synaptic Density Imaging with ¹¹ C-UCB-J Detects Treatment Effects of Saracatinib in a Mouse Model of Alzheimer Disease. Journal of Nuclear Medicine, 2019, 60, 1780-1786.	5.0	57
31	PTSD is associated with neuroimmune suppression: evidence from PET imaging and postmortem transcriptomic studies. Nature Communications, 2020, 11, 2360.	12.8	56
32	Synaptic density and cognitive performance in Alzheimer's disease: A PET imaging study with [¹¹ C]UCBâ€J. Alzheimer's and Dementia, 2022, 18, 2527-2536.	0.8	55
33	Evaluation of the agonist PET radioligand [11C]GR103545 to image kappa opioid receptor in humans: Kinetic model selection, test–retest reproducibility and receptor occupancy by the antagonist PF-04455242. Neurolmage, 2014, 99, 69-79.	4.2	54
34	Anti-edema and antioxidant combination therapy for ischemic stroke via glyburide-loaded betulinic acid nanoparticles. Theranostics, 2019, 9, 6991-7002.	10.0	54
35	Association of Aβ deposition and regional synaptic density in early Alzheimer's disease: a PET imaging study with [11C]UCB-J. Alzheimer's Research and Therapy, 2021, 13, 11.	6.2	53
36	A Positron Emission Tomography Radioligand for the in Vivo Labeling of Metabotropic Glutamate 1 Receptor:Â (3-Ethyl-2-[11C]methyl-6-quinolinyl)(cis- 4-methoxycyclohexyl)methanone. Journal of Medicinal Chemistry, 2005, 48, 5096-5099.	6.4	52

#	Article	IF	CITATIONS
37	Reduced synaptic vesicle protein 2A binding in temporal lobe epilepsy: A [¹¹ C]UCBâ€J positron emission tomography study. Epilepsia, 2020, 61, 2183-2193.	5.1	51
38	In vivo evidence of lower synaptic vesicle density in schizophrenia. Molecular Psychiatry, 2021, 26, 7690-7698.	7.9	51
39	Reductions in Brain 5-HT1B Receptor Availability in Primarily Cocaine-Dependent Humans. Biological Psychiatry, 2014, 76, 816-822.	1.3	50
40	Receptor Occupancy of the Â-Opioid Antagonist LY2456302 Measured with Positron Emission Tomography and the Novel Radiotracer 11C-LY2795050. Journal of Pharmacology and Experimental Therapeutics, 2016, 356, 260-266.	2.5	47
41	PET imaging of α7 nicotinic acetylcholine receptors: a comparative study of [18F]ASEM and [18F]DBT-10 in nonhuman primates, and further evaluation of [18F]ASEM in humans. European Journal of Nuclear Medicine and Molecular Imaging, 2017, 44, 1042-1050.	6.4	47
42	InÂVivo Reactive Oxygen Species Detection With a Novel Positron Emission Tomography Tracer, 18F-DHMT, Allows for Early Detection of Anthracycline-Induced Cardiotoxicity in Rodents. JACC Basic To Translational Science, 2018, 3, 378-390.	4.1	46
43	A singleâ€center, openâ€label positron emission tomography study to evaluate brivaracetam and levetiracetam synaptic vesicle glycoprotein 2A binding in healthy volunteers. Epilepsia, 2019, 60, 958-967.	5.1	45
44	PET Imaging for Early Detection of Alzheimer's Disease. PET Clinics, 2017, 12, 329-350.	3.0	44
45	Quantitative Analysis of [11C]-Erlotinib PET Demonstrates Specific Binding for Activating Mutations of the EGFR Kinase Domain. Neoplasia, 2013, 15, 1347-1353.	5.3	43
46	Imaging Nicotine- and Amphetamine-Induced Dopamine Release in Rhesus Monkeys with [11C]PHNO vs [11C]raclopride PET. Neuropsychopharmacology, 2014, 39, 866-874.	5.4	43
47	Age-related changes in binding of the D2/3 receptor radioligand [11C](+)PHNO in healthy volunteers. NeuroImage, 2016, 130, 241-247.	4.2	43
48	Comparison of [¹¹ C]UCB-J and [¹⁸ F]FDG PET in Alzheimer's disease: A tracer kinetic modeling study. Journal of Cerebral Blood Flow and Metabolism, 2021, 41, 2395-2409.	4.3	43
49	Kinetic Modeling of 11C-LY2795050, A Novel Antagonist Radiotracer for PET Imaging of the Kappa Opioid Receptor in Humans. Journal of Cerebral Blood Flow and Metabolism, 2014, 34, 1818-1825.	4.3	42
50	High-resolution imaging of brain 5-HT1B receptors in the rhesus monkey using [11C]P943. Nuclear Medicine and Biology, 2010, 37, 205-214.	0.6	40
51	Development of Effective PET and SPECT Imaging Agents for the Serotonin Transporter: Has a Twenty-Year Journey Reached its Destination?. Current Topics in Medicinal Chemistry, 2010, 10, 1499-1526.	2.1	39
52	A new positron emission tomography imaging agent for the serotonin transporter: synthesis, pharmacological characterization, and kinetic analysis of [11C]2-[2-(dimethylaminomethyl)phenylthio]-5-fluoromethylphenylamine ([11C]AFM). Nuclear Medicine and Biology, 2004, 31, 543-556.	0.6	38
53	Parametric Imaging and Test–Retest Variability of ¹¹ C-(+)-PHNO Binding to D ₂ /D ₃ Dopamine Receptors in Humans on the High-Resolution Research Tomograph PET Scanner. Journal of Nuclear Medicine, 2014, 55, 960-966.	5.0	38
54	Synthesis and in vivo evaluation of [18F]UCB-J for PET imaging of synaptic vesicle glycoprotein 2A (SV2A). European Journal of Nuclear Medicine and Molecular Imaging, 2019, 46, 1952-1965.	6.4	38

#	Article	IF	CITATIONS
55	PET imaging reveals lower kappa opioid receptor availability in alcoholics but no effect of age. Neuropsychopharmacology, 2018, 43, 2539-2547.	5.4	37
56	High Single Doses of Radiation May Induce Elevated Levels of Hypoxia in Early-Stage Non-Small Cell Lung Cancer Tumors. International Journal of Radiation Oncology Biology Physics, 2018, 102, 174-183.	0.8	36
57	Kappa-opioid receptors, dynorphin, and cocaine addiction: a positron emission tomography study. Neuropsychopharmacology, 2019, 44, 1720-1727.	5.4	36
58	Test–Retest Reproducibility of Binding Parameters in Humans with ¹¹ C-LY2795050, an Antagonist PET Radiotracer for the κ Opioid Receptor. Journal of Nuclear Medicine, 2015, 56, 243-248.	5.0	35
59	First-in-Human Assessment of ¹¹ C-LSN3172176, an M1 Muscarinic Acetylcholine Receptor PET Radiotracer. Journal of Nuclear Medicine, 2021, 62, 553-560.	5.0	35
60	In Vivo Imaging of the Metabotropic Glutamate Receptor 1 (mGluR1) with Positron Emission Tomography: Recent Advance and Perspective. Current Medicinal Chemistry, 2013, 21, 113-123.	2.4	34
61	Age-Related Change in 5-HT ₆ Receptor Availability in Healthy Male Volunteers Measured with ¹¹ C-GSK215083 PET. Journal of Nuclear Medicine, 2018, 59, 1445-1450.	5.0	34
62	Synthesis and Preclinical Evaluation of an ¹⁸ F-Labeled Synaptic Vesicle Glycoprotein 2A PET Imaging Probe: [¹⁸ F]SynVesT-2. ACS Chemical Neuroscience, 2020, 11, 592-603.	3.5	34
63	Preliminary in vivo evidence of lower hippocampal synaptic density in cannabis use disorder. Molecular Psychiatry, 2021, 26, 3192-3200.	7.9	32
64	Determination of In Vivo <i>B</i> _{max} and <i>K</i> _d for ¹¹ C-GR103545, an Agonist PET Tracer for κ-Opioid Receptors: A Study in Nonhuman Primates. Journal of Nuclear Medicine, 2013, 54, 600-608.	5.0	31
65	PET imaging of mGluR5 in Alzheimer's disease. Alzheimer's Research and Therapy, 2020, 12, 15.	6.2	29
66	Novel ¹⁸ F-Labeled κ-Opioid Receptor Antagonist as PET Radiotracer: Synthesis and In Vivo Evaluation of ¹⁸ F-LY2459989 in Nonhuman Primates. Journal of Nuclear Medicine, 2018, 59, 140-146.	5.0	28
67	Cortical β-amyloid burden, gray matter, and memory in adults at varying APOE ε4 risk for Alzheimer's disease. Neurobiology of Aging, 2018, 61, 207-214.	3.1	28
68	Binding of the synaptic vesicle radiotracer [¹¹ C]UCB-J is unchanged during functional brain activation using a visual stimulation task. Journal of Cerebral Blood Flow and Metabolism, 2021, 41, 1067-1079.	4.3	28
69	First-in-Human Assessment of the Novel PDE2A PET Radiotracer ¹⁸ F-PF-05270430. Journal of Nuclear Medicine, 2016, 57, 1388-1395.	5.0	27
70	Neuroprotective effects of stemazole in the MPTP-induced acute model of Parkinson's disease: Involvement of the dopamine system. Neuroscience Letters, 2016, 616, 152-159.	2.1	27
71	The Kappa Opioid Receptor Is Associated With Naltrexone-Induced Reduction of Drinking and Craving. Biological Psychiatry, 2019, 86, 864-871.	1.3	27
72	An Improved Antagonist Radiotracer for the κ-Opioid Receptor: Synthesis and Characterization of 11C-LY2459989. Journal of Nuclear Medicine, 2014, 55, 1185-1191.	5.0	26

#	Article	IF	CITATIONS
73	Imaging human brown adipose tissue under room temperature conditions with 11C-MRB, a selective norepinephrine transporter PET ligand. Metabolism: Clinical and Experimental, 2015, 64, 747-755.	3.4	25
74	Preliminary In Vivo Evidence of Reduced Synaptic Density in Human Immunodeficiency Virus (HIV) Despite Antiretroviral Therapy. Clinical Infectious Diseases, 2021, 73, 1404-1411.	5.8	25
75	Association of entorhinal cortical tau deposition and hippocampal synaptic density in older individuals with normal cognition and early Alzheimer's disease. Neurobiology of Aging, 2022, 111, 44-53.	3.1	25
76	PET Imaging Evaluation of Four σ ₁ Radiotracers in Nonhuman Primates. Journal of Nuclear Medicine, 2017, 58, 982-988.	5.0	24
77	1-(4-[¹⁸ F]Fluorobenzyl)-4-[(tetrahydrofuran-2-yl)methyl]piperazine: A Novel Suitable Radioligand with Low Lipophilicity for Imaging Ïf ₁ Receptors in the Brain. Journal of Medicinal Chemistry, 2017, 60, 4161-4172.	6.4	24
78	Imaging sigma receptors in the brain: New opportunities for diagnosis of Alzheimer's disease and therapeutic development. Neuroscience Letters, 2019, 691, 3-10.	2.1	24
79	Synthesis and pharmacological characterization of a new PET ligand for the serotonin transporter: [11C]5-bromo-2-[2-(dimethylaminomethylphenylsulfanyl)]phenylamine ([11C]DAPA). Nuclear Medicine and Biology, 2002, 29, 741-751.	0.6	23
80	Preparation of the metabotropic glutamate receptor 5 (mGluR5) PET tracer [18 F]FPEB for human use: An automated radiosynthesis and a novel one-pot synthesis of its radiolabeling precursor. Applied Radiation and Isotopes, 2014, 94, 349-354.	1.5	23
81	Fluorine-18-Labeled Antagonist for PET Imaging of Kappa Opioid Receptors. ACS Chemical Neuroscience, 2017, 8, 12-16.	3.5	23
82	Preclinical In Vitro and In Vivo Characterization of Synaptic Vesicle 2A–Targeting Compounds Amenable to F-18 Labeling as Potential PET Radioligands for Imaging of Synapse Integrity. Molecular Imaging and Biology, 2020, 22, 832-841.	2.6	23
83	Assessment of test-retest reproducibility of [18F]SynVesT-1, a novel radiotracer for PET imaging of synaptic vesicle glycoprotein 2A. European Journal of Nuclear Medicine and Molecular Imaging, 2021, 48, 1327-1338.	6.4	23
84	A PET imaging agent with fast kinetics: synthesis and in vivo evaluation of the serotonin transporter and Biology, 2004, 31, 727-738.	0.6	22
85	Evaluation of PET Brain Radioligands for Imaging Pancreatic $\hat{1}^2$ -Cell Mass: Potential Utility of 11C-(+)-PHNO. Journal of Nuclear Medicine, 2018, 59, 1249-1254.	5.0	22
86	Social status and demographic effects of the kappa opioid receptor: a PET imaging study with a novel agonist radiotracer in healthy volunteers. Neuropsychopharmacology, 2019, 44, 1714-1719.	5.4	22
87	Epibatidine analogues as selective ligands for the αxβ2-containing subtypes of nicotinic acetylcholine receptors. Bioorganic and Medicinal Chemistry Letters, 2005, 15, 4385-4388.	2.2	21
88	The new PET imaging agent [11C]AFE is a selective serotonin transporter ligand with fast brain uptake kinetics. Nuclear Medicine and Biology, 2004, 31, 983-994.	0.6	20
89	PET imaging evaluation of [18F]DBT-10, a novel radioligand specific to α7 nicotinic acetylcholine receptors, in nonhuman primates. European Journal of Nuclear Medicine and Molecular Imaging, 2016, 43, 537-547.	6.4	20
90	Development and In Vivo Evaluation of a κ-Opioid Receptor Agonist as a PET Radiotracer with Superior Imaging Characteristics. Journal of Nuclear Medicine, 2019, 60, 1023-1030.	5.0	20

#	Article	IF	CITATIONS
91	Development of [89Zr]ZrDFO-amivantamab bispecific to EGFR and c-MET for PET imaging of triple-negative breast cancer. European Journal of Nuclear Medicine and Molecular Imaging, 2021, 48, 383-394.	6.4	20
92	Quantification of SV2A Binding in Rodent Brain Using [18F]SynVesT-1 and PET Imaging. Molecular Imaging and Biology, 2021, 23, 372-381.	2.6	20
93	Synthesis of [18 F]FMISO in a flow-through microfluidic reactor: Development and clinical application. Nuclear Medicine and Biology, 2015, 42, 578-584.	0.6	19
94	PET Imaging of Pancreatic Dopamine D ₂ and D ₃ Receptor Density with ¹¹ C-(+)-PHNO in Type 1 Diabetes. Journal of Nuclear Medicine, 2020, 61, 570-576.	5.0	19
95	Simplified Quantification of ¹¹ C-UCB-J PET Evaluated in a Large Human Cohort. Journal of Nuclear Medicine, 2021, 62, 418-421.	5.0	19
96	Optimized and Automated Radiosynthesis of [18F]DHMT for Translational Imaging of Reactive Oxygen Species with Positron Emission Tomography. Molecules, 2016, 21, 1696.	3.8	18
97	18 F-Labeled indole-based analogs as highly selective radioligands for imaging sigma-2 receptors in the brain. Bioorganic and Medicinal Chemistry, 2017, 25, 3792-3802.	3.0	18
98	Tracer Kinetic Modeling of [¹¹ C]AFM, a New PET Imaging Agent for the Serotonin Transporter. Journal of Cerebral Blood Flow and Metabolism, 2013, 33, 1886-1896.	4.3	17
99	Synthesis and evaluation of a 18F-labeled spirocyclic piperidine derivative as promising $lf1$ receptor imaging agent. Bioorganic and Medicinal Chemistry, 2014, 22, 5270-5278.	3.0	17
100	Evaluation of [18 F]-(-)-norchlorofluorohomoepibatidine ([18 F]-(-)-NCFHEB) as a PET radioligand to image the nicotinic acetylcholine receptors in non-human primates. Nuclear Medicine and Biology, 2015, 42, 570-577.	0.6	17
101	Quantitative Analysis of Dynamic ¹²³ I-mIBG SPECT Imaging Data in Healthy Humans with a Population-Based Metabolite Correction Method. Journal of Nuclear Medicine, 2016, 57, 1226-1232.	5.0	17
102	Quantification of Tumor Hypoxic Fractions Using Positron Emission Tomography with [18F]Fluoromisonidazole ([18F]FMISO) Kinetic Analysis and Invasive Oxygen Measurements. Molecular Imaging and Biology, 2017, 19, 893-902.	2.6	17
103	Evaluation of ¹¹ C-LSN3172176 as a Novel PET Tracer for Imaging M ₁ Muscarinic Acetylcholine Receptors in Nonhuman Primates. Journal of Nuclear Medicine, 2019, 60, 1147-1153.	5.0	17
104	In vivo 5-HT6 and 5-HT2A receptor availability in antipsychotic treated schizophrenia patients vs. unmedicated healthy humans measured with [11C]GSK215083 PET. Psychiatry Research - Neuroimaging, 2020, 295, 111007.	1.8	17
105	Occupancy of the kappa opioid receptor by naltrexone predicts reduction in drinking and craving. Molecular Psychiatry, 2021, 26, 5053-5060.	7.9	17
106	Evaluation of the Lysophosphatidic Acid Receptor Type 1 Radioligand ¹¹ C-BMT-136088 for Lung Imaging in Rhesus Monkeys. Journal of Nuclear Medicine, 2018, 59, 327-333.	5.0	16
107	Quantification of Positron Emission Tomography Data Using Simultaneous Estimation of the Input Function: Validation with Venous Blood and Replication of Clinical Studies. Molecular Imaging and Biology, 2019, 21, 926-934.	2.6	16
108	A metabolically stable PET tracer for imaging synaptic vesicle protein 2A: synthesis and preclinical characterization of [18F]SDM-16. European Journal of Nuclear Medicine and Molecular Imaging, 2022, 49, 1482-1496.	6.4	16

#	Article	IF	CITATIONS
109	Lower prefrontal cortical synaptic vesicle binding in cocaine use disorder: An exploratory ¹¹ Câ€UCBâ€J positron emission tomography study in humans. Addiction Biology, 2022, 27, e13123.	2.6	16
110	Neuroprotective Effects of Jitai Tablet, a Traditional Chinese Medicine, on the MPTP-Induced Acute Model of Parkinson's Disease: Involvement of the Dopamine System. Evidence-based Complementary and Alternative Medicine, 2014, 2014, 1-9.	1.2	15
111	A Promising PET Tracer for Imaging of α7 Nicotinic Acetylcholine Receptors in the Brain: Design, Synthesis, and in Vivo Evaluation of a Dibenzothiophene-Based Radioligand. Molecules, 2015, 20, 18387-18421.	3.8	13
112	Preclinical Evaluation of ¹⁸ F-PF-05270430, a Novel PET Radioligand for the Phosphodiesterase 2A Enzyme. Journal of Nuclear Medicine, 2016, 57, 1448-1453.	5.0	13
113	The Effect of Treatment with Guanfacine, an Alpha2 Adrenergic Agonist, on Dopaminergic Tone in Tobacco Smokers: An [11C]FLB457 PET Study. Neuropsychopharmacology, 2018, 43, 1052-1058.	5.4	12
114	A Novel ¹⁸ F-Labeled Radioligand for Positron Emission Tomography Imaging of 11β-Hydroxysteroid Dehydrogenase (11I²-HSD1): Synthesis and Preliminary Evaluation in Nonhuman Primates. ACS Chemical Neuroscience, 2019, 10, 2450-2458.	3.5	12
115	Synthesis of potent and selective serotonin 5-HT1B receptor ligands. Bioorganic and Medicinal Chemistry Letters, 2005, 15, 4786-4789.	2.2	11
116	Enhanced selective serotonin re-uptake inhibitors as antidepressants: 2004 – 2006. Expert Opinion on Therapeutic Patents, 2007, 17, 889-907.	5.0	11
117	Imaging the Enzyme 11β-Hydroxysteroid Dehydrogenase Type 1 with PET: Evaluation of the Novel Radiotracer ¹¹ C-AS2471907 in Human Brain. Journal of Nuclear Medicine, 2019, 60, 1140-1146.	5.0	11
118	Cortical abnormalities of synaptic vesicle protein 2A in focal cortical dysplasia type II identified in vivo with 18F-SynVesT-1 positron emission tomography imaging. European Journal of Nuclear Medicine and Molecular Imaging, 2022, 49, 3482-3491.	6.4	11
119	Measurement of <i>B</i> _{max} and <i>K</i> _d with the Glycine Transporter 1 Radiotracer ¹⁸ F-MK6577 using a Novel Multi-Infusion Paradigm. Journal of Cerebral Blood Flow and Metabolism, 2015, 35, 2001-2009.	4.3	10
120	Longitudinal changes of dopamine transporters in heroin users during abstinence. Psychopharmacology, 2015, 232, 3391-3401.	3.1	10
121	First in-human PET study and kinetic evaluation of [¹⁸ F]AS2471907 for imaging 11β-hydroxysteroid dehydrogenase type 1. Journal of Cerebral Blood Flow and Metabolism, 2020, 40, 695-704.	4.3	10
122	Positron Emission Tomography Imaging Evaluation of a Novel 18F-Labeled Sigma-1 Receptor Radioligand in Cynomolgus Monkeys. ACS Chemical Neuroscience, 2020, 11, 1673-1681.	3.5	10
123	Preclinical Advances in Theranostics for the Different Molecular Subtypes of Breast Cancer. Frontiers in Pharmacology, 2021, 12, 627693.	3.5	10
124	Effect of age on brain metabotropic glutamate receptor subtype 5 measured with [18F]FPEB PET. NeuroImage, 2021, 238, 118217.	4.2	10
125	Imaging brain cortisol regulation in PTSD with a target for 11β-hydroxysteroid dehydrogenase type 1. Journal of Clinical Investigation, 2021, 131, .	8.2	10
126	Validation of SV2A-Targeted PET Imaging for Noninvasive Assessment of Neuroendocrine Differentiation in Prostate Cancer. International Journal of Molecular Sciences, 2021, 22, 13085.	4.1	10

#	Article	IF	CITATIONS
127	Synthesis and characterization of two pet radioligands for the metabotropic glutamate 1 (mGlu1) receptor. Synapse, 2012, 66, 1002-1014.	1.2	9
128	Bridging from Brain to Tumor Imaging: (S)-(â^')- and (R)-(+)-[18F]Fluspidine for Investigation of Sigma-1 Receptors in Tumor-Bearing Mice. Molecules, 2018, 23, 702.	3.8	9
129	Novel Kappa Opioid Receptor Agonist as Improved PET Radiotracer: Development and in Vivo Evaluation. Molecular Pharmaceutics, 2019, 16, 1523-1531.	4.6	9
130	Body Mass Index and Age Effects on Brain 11β-Hydroxysteroid Dehydrogenase Type 1: a Positron Emission Tomography Study. Molecular Imaging and Biology, 2020, 22, 1124-1131.	2.6	9
131	Inverse changes in raphe and cortical 5â€HT 1B receptor availability after acute tryptophan depletion in healthy human subjects. Synapse, 2020, 74, e22159.	1.2	9
132	Separating dopamine D2 and D3 receptor sources of [11C]-(+)-PHNO binding potential: Independent component analysis of competitive binding. NeuroImage, 2020, 214, 116762.	4.2	9
133	Effects of Jitai Tablet, A Traditional Chinese Medicine, on Spontaneous Withdrawal Symptoms and Modulation of Dopaminergic Functions in Morphine-Dependent Rats. Phytotherapy Research, 2015, 29, 687-694.	5.8	8
134	A multi species evaluation of the radiation dosimetry of [11 C]erlotinib, the radiolabeled analog of a clinically utilized tyrosine kinase inhibitor. Nuclear Medicine and Biology, 2017, 47, 56-61.	0.6	8
135	The Search for a Subtype-Selective PET Imaging Agent for the GABA _A Receptor Complex: Evaluation of the Radiotracer [¹¹ C]ADO in Nonhuman Primates. Molecular Imaging, 2017, 16, 153601211773125.	1.4	8
136	Tobacco Smoking in People Is Not Associated with Altered 18-kDa Translocator Protein Levels: A PET Study. Journal of Nuclear Medicine, 2020, 61, 1200-1204.	5.0	8
137	Human adult and adolescent biodistribution and dosimetry of the synaptic vesicle glycoprotein 2A radioligand 11C-UCB-J. EJNMMI Research, 2020, 10, 83.	2.5	8
138	Characterization in nonhuman primates of (R)-[18F]OF-Me-NB1 and (S)-[18F]OF-Me-NB1 for imaging the GluN2B subunits of the NMDA receptor. European Journal of Nuclear Medicine and Molecular Imaging, 2022, , 1.	6.4	8
139	Evaluation of (â€)â€{ ¹⁸ <scp>F]F</scp> lubatineâ€specific binding: Implications for reference region approaches. Synapse, 2018, 72, e22016.	1.2	7
140	Binge alcohol use is not associated with alterations in striatal dopamine receptor binding or dopamine release. Drug and Alcohol Dependence, 2019, 205, 107627.	3.2	7
141	Imaging Pituitary Vasopressin 1B Receptor in Humans with the PET Radiotracer ¹¹ C-TASP699. Journal of Nuclear Medicine, 2022, 63, 609-614.	5.0	7
142	Comparison of three novel radiotracers for GluN2B-containing NMDA receptors in non-human primates: <i>(R)</i> -[¹¹ C]NR2B-Me, <i>(R)</i> -[¹⁸ F]of-Me-NB1, and <i>(S)</i> -[¹⁸ F]of-NB1. Journal of Cerebral Blood Flow and Metabolism, 2022, 42, 1398-1409.	4.3	7
143	Discovery and development of brain-penetrant 18F-labeled radioligands for neuroimaging of the sigma-2 receptors. Acta Pharmaceutica Sinica B, 2022, 12, 1406-1415.	12.0	6
144	Synthesis and evaluation of new 1-oxa-8-azaspiro[4.5]decane derivatives as candidate radioligands for sigma-1 receptors. Bioorganic and Medicinal Chemistry, 2020, 28, 115560.	3.0	6

#	Article	IF	CITATIONS
145	Synthesis and characterization of the two enantiomers of a chiral sigma-1 receptor radioligand: (S)-(+)- and (R)-(-)-[18F]FBFP. Chinese Chemical Letters, 2022, 33, 3543-3548.	9.0	6
146	Nicotine and Nicotine Abstinence Do Not Interfere with GABA _A Receptor Neuroadaptations During Alcohol Abstinence. Alcoholism: Clinical and Experimental Research, 2016, 40, 698-705.	2.4	5
147	A modification to improve the reliability of <scp>[¹¹C]CN^{â^'}</scp> production in the <scp>GE</scp> radiochemistry system. Journal of Labelled Compounds and Radiopharmaceuticals, 2017, 60, 592-595.	1.0	5
148	Quantitative projection of human brain penetration of the H ₃ antagonist PF-03654746 by integrating rat-derived brain partitioning and PET receptor occupancy. Xenobiotica, 2017, 47, 119-126.	1.1	5
149	Automated radiosynthesis of [18F]FBEM, a sulfhydryl site specific labeling agent for peptides and proteins. Applied Radiation and Isotopes, 2018, 140, 294-299.	1.5	5
150	Feasibility study of PET dynamic imaging of [18F]DHMT for quantification of reactive oxygen species in the myocardium of large animals. Journal of Nuclear Cardiology, 2022, 29, 216-225.	2.1	5
151	PET Imaging Estimates of Regional Acetylcholine Concentration Variation in Living Human Brain. Cerebral Cortex, 2021, 31, 2787-2798.	2.9	5
152	Recently Abstinent Smokers Exhibit Mood-Associated Dopamine Dysfunction in the Ventral Striatum Compared to Nonsmokers: A [11C]-(+)-PHNO PET Study. Nicotine and Tobacco Research, 2022, 24, 745-752.	2.6	5
153	Comparative evaluation of two glycine transporter 1 radiotracers [11C]GSK931145 and [18F]MK-6577 in baboons. Synapse, 2016, 70, 112-120.	1.2	4
154	PET Imaging in Animal Models of Alzheimer's Disease. Frontiers in Neuroscience, 2022, 16, .	2.8	4
155	Imaging the fetal nonhuman primate brain with SV2A positron emission tomography (PET). European Journal of Nuclear Medicine and Molecular Imaging, 2022, 49, 3679-3691.	6.4	4
156	Protective and restorative effects of the traditional Chinese medicine Jitai tablet against methamphetamine-induced dopaminergic neurotoxicity. BMC Complementary and Alternative Medicine, 2018, 18, 76.	3.7	3
157	Feasibility of imaging synaptic density in the human spinal cord using [11C]UCB-J PET. EJNMMI Physics, 2022, 9, 32.	2.7	3
158	¹⁸ F‣abeled benzylpiperazine derivatives as highly selective ligands for imaging σ ₁ receptor with positron emission tomography. Journal of Labelled Compounds and Radiopharmaceuticals, 2019, 62, 425-437.	1.0	2
159	Association between cerebrospinal fluid biomarkers of neurodegeneration and PET measurements of synaptic density in Alzheimer's disease. Alzheimer's and Dementia, 2020, 16, e044211.	0.8	2
160	Further Investigation of Synaptic Vesicle Protein 2A (SV2A) Ligands Designed for Positron Emission Tomography and Single-Photon Emission Computed Tomography Imaging: Synthesis and Structure–Activity Relationship of Substituted Pyridinylmethyl-4-(3,5-difluorophenyl)pyrrolidin-2-ones. ACS Omega, 2021, 6, 27676-27683.	3.5	2
161	Differences in the association between kappa opioid receptors and pain among Black and White adults with alcohol use disorders. Alcoholism: Clinical and Experimental Research, 2022, 46, 1348-1357.	2.4	2
162	In vivo measurement of widespread synaptic loss and associated tau accumulation in early Alzheimer's disease. Alzheimer's and Dementia, 2020, 16, e037791.	0.8	1

#	Article	IF	CITATIONS
163	Validation of a simplified tissueâ€toâ€reference ratio measurement using SUVR for the assessment of synaptic density alterations in Alzheimer's disease using [11 C]UCBâ€J PET. Alzheimer's and Dementia, 2020, 16, e045928.	0.8	1
164	Dopamine D2/3 receptor availability in cocaine use disorder individuals with obesity as measured by [11C]PHNO PET. Drug and Alcohol Dependence, 2021, 220, 108514.	3.2	1
165	P2â€365: PET IMAGING OF SYNAPTIC DENSITY (SYNAPTIC VESICLE GLYCOPROTEIN 2A, SV2A) IN ALZHEIMER'S DISEASE: INITIAL EXPERIENCE. Alzheimer's and Dementia, 2018, 14, P832.	0.8	0
166	ICâ€Pâ€183: PET IMAGING OF SYNAPTIC DENSITY (SYNAPTIC VESICLE GLYCOPROTEIN 2A, SV2A) IN ALZHEIMER'S DISEASE: INITIAL EXPERIENCE. Alzheimer's and Dementia, 2018, 14, P152.	0.8	0
167	P4â€481: ASSOCIATION BETWEEN ENTORHINAL CORTICAL TAU ACCUMULATION AND HIPPOCAMPAL SYNAPTIC DENSITY IN OLDER INDIVIDUALS WITH NORMAL COGNITION AND EARLY ALZHEIMER'S DISEASE: PRELIMINARY EXPERIENCE. Alzheimer's and Dementia, 2019, 15, P1497.	0.8	0
168	ICâ€Pâ€140: ASSOCIATION BETWEEN MGLUR5 AND SYNAPTIC DENSITY: A MULTIâ€TRACER STUDY IN HEALTHY A AND ALZHEIMER'S DISEASE. Alzheimer's and Dementia, 2019, 15, P115.	AGING	0
169	PBR28 Brain PET imaging with lipopolysaccharide challenge for the study of microglia function in Alzheimer's disease. Alzheimer's and Dementia, 2020, 16, e037792.	0.8	Ο
170	11Câ€PBR28 brain PET imaging with lipopolysaccharide challenge for the study of microglia function in Alzheimer's disease. Alzheimer's and Dementia, 2020, 16, e043584.	0.8	0
171	Association between cerebral amyloid accumulation and synaptic density in Alzheimer's disease: A multitracer PET study. Alzheimer's and Dementia, 2020, 16, e043631.	0.8	0
172	Social Rank, Behavioral Phenotypes and Kappa Opioid Receptor: PET Imaging Studies of Socially Housed Female and Male Monkey Models of Cocaine Use Disorder. FASEB Journal, 2021, 35, .	0.5	0
173	Translational PET Imaging of Spinal Cord Injury with the Serotonin Transporter Tracer [11C]AFM. Molecular Imaging and Biology, 2022 1.	2.6	0